analytical chemistry

ARTICLE

pubs.acs.org/ac

Three Different Approaches for the Clarification of the Interactions between Lipoproteins and Chondroitin-6-sulfate

Katriina Lipponen,[†] Patricia W. Stege,[†,‡] Geraldine Cilpa,[†] Jörgen Samuelsson,[§] Torgny Fornstedt,[§,∥] and Marja-Liisa Riekkola*[,†]

[†]Laboratory of Analytical Chemistry, Department of Chemistry, P.O. Box 55, FIN-00014, University of Helsinki, Finland

[‡]INQUISAL, Laboratory of Analytical Chemistry, Department of Chemistry, D5700BWS, National University of San Luis-CONICET, San Luis, Argentina

[§]Analytical Chemistry, Department of Chemistry and Biomedical Sciences, Karlstad University, SE-651 88 Karlstad, Sweden

[∥]Department of Physical and Analytical Chemistry, Uppsala University, BMC Box 599, SE-751 24 Uppsala, Sweden

Supporting Information

ABSTRACT: Two different experimental approaches were used for obtaining a comprehensive view and understanding of the interactions between apolipoprotein B-100 (ApoB-100) of low-density lipoprotein and apolipoprotein E (ApoE) of high-density lipoprotein and chondroitin-6-sulfate (C6S) of arterial proteoglycan. The techniques employed were partial filling affinity capillary electrophoresis (PF-ACE) and continuous flow quartz crystal microbalance (QCM). In addition, molecular dynamic (MD) simulations were used to provide a supportive visual insight into the interaction mechanism. A new tool for analysis of QCM-data was utilized, i.e., adsorption energy distribution calculations, which allowed a deeper understanding of the interactions, especially at different temperatures. The PF-ACE technique probed mainly the strong adsorption interactions whereas in the MD calculations short- and long-range interactions could be distinguished. Although there are differences in the techniques, a pretty good agreement was achieved between the three approaches for the interaction of 19 amino acid peptide of ApoB with C6S giving log affinity constants of 4.66 by QCM, 5.02 by PF-ACE, and 7.39 by MD, and for 15 amino acid peptide of ApoE with C6S 5.34 by QCM, 5.28 by PT-ACE, and 4.60 by MD at physiological temperature 37.0 °C.

The intimal extracellular matrix (ECM) forms an organized, tight network, and the retention of lipoproteins by extracellular matrix components is believed to be critical in the pathogenesis of atherosclerosis.[1−3] Among ECM components especially proteoglycans (PG) are well-known for their ability to retain lipoproteins in the arterial wall by interacting with negatively charged groups on the proteoglycan side chains with clusters of positively charged amino acid residues on apolipoprotein B (ApoB) and apolipoprotein E (ApoE).[4,5] Among the linear glycosaminoglycans (GAG), chondroitin-6-sulfate (C6S) has been proven to play an important role in the interaction with low-density lipoprotein (LDL) resulting in the development of atherosclerotic diseases.[4,6−8] The hypothetic mechanism, in particular, suggests that interactions between C6S and LDL are mediated by specific peptide fragments of the major apolipoprotein ApoB-100 of LDL. ApoB-100 with molecular mass of about 512 kDa is known to contain more than 4000 amino acid residues. Smaller ApoE that is one of the apolipoprotein components of high-density lipoprotein (HDL) includes also nowadays well-defined domains.

Innumerable studies have been carried out aiming at comprehending lipoproteins modality of accumulation and modification in the arteries. Frontal elution affinity chromatographic study on the interaction of LDL and ApoB-100 synthetic peptides with agarose-arterial PG[6] indicated that at least three peptide fragments of ApoB-100 have measurable interactions. Among them, highly positive 19 amino acid peptide fragment domain 3359−3377 (charge +6) of ApoB-100 with arginine and lysine amino acid rich components experienced the highest affinity toward C6S. The fact that this residue is part of the LDL receptor domain has been regarded as the basis for the findings that sulfated GAG compete for the association of ApoB/ApoE containing lipoproteins with the receptor. The residue 136−150 of ApoE that is similar in charge distribution to that of the residues 3359−3377 of ApoB has been identified as a heparin binding site. The latter being a highly sulfated GAG. This similar charge distribution is prone to explain association of ApoE with the arterial PG.

A complete understanding of atherosclerosis at the molecular level requires unraveling of the changes of molecular interactions during atherogenesis. These nanoscale interactions influence the metabolism of the lipoprotein particles in the arterial wall by affecting the interactions of lipoproteins with the components of the ECM. Evidence from many biochemical studies supports the hypothesis that HDL particles protect against the development of atherosclerotic coronary heart disease due to their role in the pathway of reverse cholesterol transport.

To get the information required for a comprehensive view on LDL and HDL interactions with C6S of the ECM, the potentials of three different approaches were clarified at physiological pH and at ambient and physiological temperatures in this work. To simplify the studies, two main peptide fragments were selected

Received: April 29, 2011
Accepted: June 7, 2011
Published: June 07, 2011

for the investigation: the 19 amino acid peptide fragment of ApoB (3359−3377) and the 15 amino acid peptide fragment of ApoE (136−150).

The first (I) approach involved the introduction of a numerical tool for analysis of quartz crystal microbalance (QCM) data, so-called adsorption energy distribution (AED) calculations. We have previously used QCM for investigating strong affinity antigen and antibody or protein/receptor interactions.[9,10] AED-calculations were recently introduced for a more reliable evaluation of adsorption in the chromatographic community,[11−13] here enabling a detailing of the degree of heterogeneity of the interactions a priori to the model fitting procedure, i.e., the different number of interactions sites, their relative abundance, and their relative different energies. More recently, AED-calculations was successfully introduced also for reliable determination of adsorption data in surface plasmon resonance analysis.[14]

The second (II) approach in this study comprised a partial-filling affinity capillary electrophoresis (PF-ACE) technique.[15] Capillary coating was needed to eliminate unwanted interactions of cationic analytes or biological components with positive net charge acting as a dispersed phase and the negative inner capillary wall. The PF-ACE method was fast allowing the determination of quite strong interactions. The third (III) approach comprised molecular dynamics (MD) simulation methods. MD simulations provide answers to questions at the molecular level that are very difficult or even impossible sometimes to approach experimentally. Potential of mean force was obtained to probe the molecular association between the peptides and C6S and for the quantitative determination of the magnitude of the interaction.

EXPERIMENTAL SECTION

General Chemicals and Materials. ApoB 19 aa and ApoE 15 aa peptide fragments synthesized at the Meilahti Protein Chemistry Facility were analyzed at the Protein Chemistry Core Facility, both at Biomedicum, University of Helsinki, Finland. C6S, 1-ethyl-3-(3-dimethylaminopropyl) carbodiimide hydrochloride (EDC), *N*-hydroxylsulfosuccinimide sodium salt (sulfo-NHS), 4-(2-hydroxyethyl)-1-piperazineethanesulfonic acid (HEPES), and ethylene diamine were purchased from Sigma-Aldrich. Phosphoric acid was purchased from VWR and NaCl from J.T.Baker.

Quartz Crystal Microbalance. *Quartz Crystal Microbalance Analysis Procedure.* The QCM experiments were performed with an Attana A100 QCM biosensor (Attana AB, Stockholm, Sweden). The crystal was sandwiched between two gold plated electrodes. An oscillating potential was applied through the electrodes to excite an acoustic wave in the crystal resulting in the shear mode oscillation. C6S was amino coupled to the LNB-carboxyl chip (Figure S-1). The binding of analyte to the surface was monitored by frequency logging, and the resulting frequency shifts (Δf) were recorded. The coating procedure and details of buffer and sample preparation are found in the Supporting Information.

Capillary Electrophoresis. *Equipment.* A Hewlett-Packard 3^D CE system (Agilent, Waldbronn, Germany) equipped with a diode array detector (detection at 200, 214, 230, and 245 nm) and an air-cooling device for the capillary was used in the capillary electrophoretic experiments. Bare fused-silica capillaries of dimensions 50 μm (i.d.) × 375 μm (o.d.) were purchased from Optronis GmbH, Kehl, Germany. The length of the capillary to the detector was 30.0 cm with a total length of 38.5 cm for all the experiments.

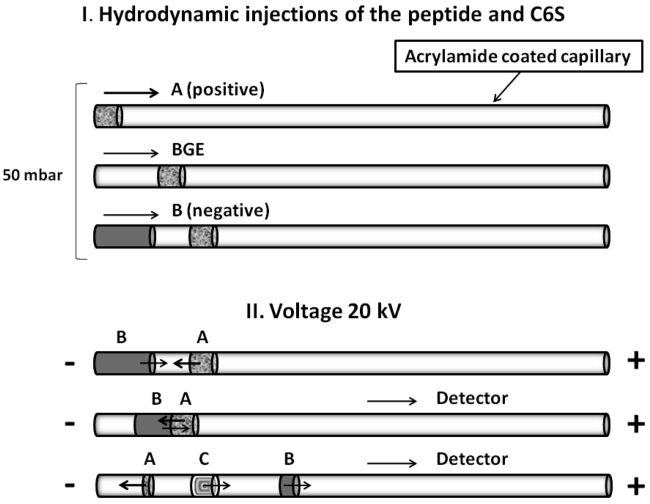

Figure 1. Schematic description of the partially filling technique in CE: (A) peptide; (B) C6S; (C) interaction between the peptide and the C6S.

Concentration of the Peptides and C6S. Standard solutions (1 mg/mL) of the peptides and C6S were diluted to 0.01 mg/mL before they were injected into the capillary.

Partial Filling Procedure. The capillaries were coated with acrylamide using a slightly modified method described by Cifuentes et al.[16] Figure 1 demonstrates the partial filling procedure used in the study. More details are found in the Supporting Information.

Theory. *Adsorption Isotherm Theory for QCM.* An adsorption isotherm describes the relationship between adsorbed and free concentration of the solute at constant and specific temperature. If the Sauerbrey relation is valid the measured QCM frequency shift is proportional to the adsorbed amount.[18] The most popular nonlinear adsorption isotherm model is the Langmuir model:

$$\Delta f = \Delta f_{max} \frac{K_a C}{1 + K_a C} \quad (1)$$

Here, Δf_{max}, C, and K_a are the maximum QCM frequency shift for monolayer saturated surfaces, the solute concentration in the buffer, and the association equilibrium constant, respectively. Adsorption is seldom homogeneous from an energetic point of view. One of the simplest models handling heterogeneous interactions is the bi-Langmuir model, assuming two independent ideal adsorption sites by adding two Langmuir terms on the right side of the equality sign:

$$\Delta f = \Delta f_{max,1} \frac{K_{a,1} C}{1 + K_{a,1} C} + \Delta f_{max,2} \frac{K_{a,2} C}{1 + K_{a,2} C} \quad (2)$$

Here, indices 1 and 2 denote the first and second adsorption sites, respectively. The second adsorption site of the bi-Langmuir model is defined as the high energy site, and the first site the low energy site, i.e., $K_{a,2} > K_{a,1}$.

The degree of heterogeneity in the adsorption can also be described by expanding the Langmuir adsorption isotherm model into a continuous distribution of independent homogeneous sites across a certain range of adsorption energies:

$$\begin{cases} \Delta f(C) = \int_{K_{min}}^{K_{max}} g(\ln K)\theta(C,K)\mathrm{d}\ln K \\ \theta(C,K) = \dfrac{KC}{1+KC} \end{cases} \quad (3)$$

dx.doi.org/10.1021/ac201110c |*Anal. Chem.* 2011, 83, 6040–6046

Here, $\theta(C, K)$ is the local adsorption model, and $g(\ln K)$ is the adsorption energy distribution. K_{min} and K_{max} are set to $1/C_{max}$ and $1/C_{min}$, respectively, where C_{min} and C_{max} are the lowest and highest sample concentration used in the QCM experiments. The AED was calculated using the expectation maximization method[11] where the integral equation is discretized to a sum and iteratively solved.

The models were selected by first analyzing the raw adsorption isotherm data using Scatchard plots, i.e., plotting $\Delta f/C$ vs Δf and AED-calculations. This considerably narrows the number of possible adsorption isotherm models prior the model fitting and statistical evaluation. Thus, we improve considerably the chance that the selected models describe the reality.

Calculation of Affinity Constants in CE Studies. The affinity constants (K_a's) of the C6S with 15 and 19 amino acid peptide were calculated according to eq 4, which is modified from equation presented in our previous report:[15]

$$K_a = \frac{t_{total}}{t_{pept} \times C_{C6S} \times V_{C6S}} \times \frac{d\Delta t}{d\Delta t_{filling}} \quad (4)$$

t_{pept} is migration time of peptide when injected without C6S in capillary, C_{C6S} is the molar concentration of C6S, V_{C6S} is the volume of C6S interacting with peptide, Δt is the change of migration time when C6S is present, $t_{filling}$ is the filling time of C6S under pressure, and t_{total} is the time of C6S to reach the detector under pressure.

Molecular Dynamic Calculations. *Molecular System and Simulation Parameters.* All selected peptide fragments were assumed to adopt α helix secondary structure in accordance with recent studies probing ApoB-100 principal PG binding site interaction with C6S.[17] Accelrys Discovery Studio (DS) 2.0 software[18] was used to build the necessary peptide and C6S chain systems. Gromacs inbuilt tool pdb2gmx was used to obtain the topology files for the peptides. All MD simulations were carried out at 310 K aligned on the experimental conditions utilizing the Gromacs 4.0.5 molecular dynamics (MD) simulation package,[19] using the GROMOS96 43a2 force field, previously used in the MD simulation of C6S polysaccharide chain.[17,20]

Each system peptide-C6S was inserted in a water box, and salt was added to neutralize and create an electrolyte solution close to physiological concentration (200 mM). The systems were then energy minimized by steepest descent followed by a conjugate gradient algorithm procedure, both after the addition of the water molecules and after the addition of ions. The temperature was maintained at 310 K and the pressure at 1 bar with help of an efficient thermostat, V-rescale,[21,22] and Berendsen barostat[23] with a coupling constant of 0.1 and 1 ps, respectively. van der Waals interactions were included with a cutoff distance of 1.4 nm as originally parametrized in GROMOS96. Particle-Mesh Ewald method was applied to take long-range electrostatic interactions into account. Real space cutoff was 1.0 nm, and the grid spacing was 0.125 nm. The MD simulations were then performed in the isothermal−isobaric NpT ensemble.

Potential of Mean Force. Potential of mean force (PMF) calculation was carried out with particular care to evaluate the interaction strength of the peptide/C6S systems. For details of the PMF construction, see Supporting Information. The dissociation constant was calculated as the inverse of the association constant K_a determined by integrating the PMF, eq 5.[24] R_c is the upper limit of association as the distance at which the integrand of eq 5 has its minimum.

$$K_a = 4\pi \int_0^c r^2 e^{-\omega(r)/RT}\, dr \quad (5)$$

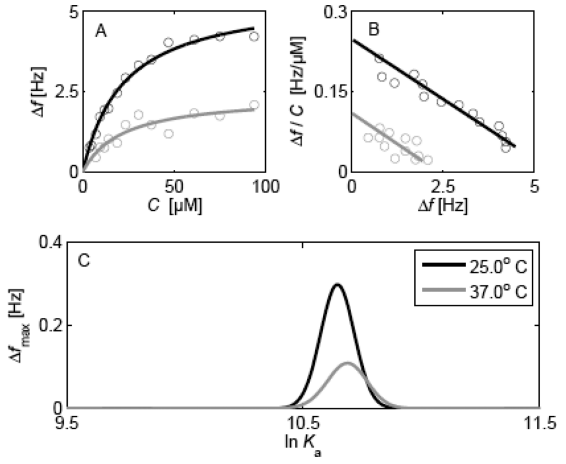

Figure 2. (A) Adsorption isotherm of 19 amino acid peptide of ApoB at 25 and 37 °C determined using QCM. (B) corresponding Scatchard plot. (C) AED-calculations for this system.

In eq 5, r is in $(1660^{1/3})$ Å unit,[25] T in Kelvin, and R, Bolzmann constant is set to 8.31×10^{-3} kJ/K/mol.

RESULTS AND DISCUSSION

Quartz Crystal Microbalance Analysis. QCM has proved to be a valuable technique for the clarification of specific interactions, such as those between antigen and antibody or protein and receptor[9,26] where usually high affinity interactions between high molecular mass molecules are in question. One of our more recent works demonstrated that weaker peptide−protein and peptide−carbohydrate interactions of more electrostatic nature can also be studied using QCM.[9] In the present study, QCM with continuous flow was exploited for a more detailed evaluation of the adsorption of 19 amino acid peptide of ApoB-100 and 15 amino acid peptide of ApoE to amino coupled C6S on LNB-carboxyl chip at two different temperatures 25.0 °C and physiological 37.0 °C. The adsorption isotherms were determined using 15 different concentrations ranging from 5 to 200 μg/mL for the 19 amino acid peptide and from 1 to 130 μg/mL for the 15 amino acid peptide. The coupling system enabled C6S to retain its biological activity essential for the interactions with peptides. As expected, the lysine and arginine residues of both peptides were involved in the binding, interacting with the negative charges of C6S.

Figure 2A presents the acquired adsorption isotherm data for 19 amino acid peptide of ApoB toward C6S at 25.0 and 37.0 °C. Figure 2B shows the corresponding Scatchard plots and Figure 2C the corresponding AED-plots. In the AED-plots, the position of the apex in the x-axis represents the adsorption energy (K_a) while the area of the distribution coefficients corresponds to Δf_{max}. The Scatchard plots (Figure 2B) at both temperatures strongly indicate that the single-site Langmuir model could probably well describe the adsorption system. However, linear Scatchard plots do not confidently state that the adsorption is described with the Langmuir model since also heterogeneous adsorption models with small energy differences between the adsorption sites will yield nearly linear Scatchard plots. This delicate problem was recently exemplified in an investigation of the adsorption of glycine peptides on 12% cross-linked agarose gel media.[27] Here, the AED analysis revealed a certain type of

Table 1. Estimated Adsorption Isotherm Parameters from AED and Model Fitting to Langmuir and Bi-Langmuir Adsorption Isotherm[a]

		AED				model fitting			
analyte	T [°C]	$\Delta f_{max,1}$ [Hz]	log $K_{a,1}$	$\Delta f_{max,2}$ [Hz]	log $K_{a,2}$	$\Delta f_{max,1}$ [Hz]	log $K_{a,1}$	$\Delta f_{max,2}$ [Hz]	log $K_{a,2}$
19 aa of ApoB	25.0	5.67	4.62	NA	NA	5.54	4.65	NA	NA
	37.0	2.43	4.64	NA	NA	2.39	4.66	NA	NA
15 aa of ApoE	25.0	NA	NA	7.82	5.42	7.77	3.91	7.00	5.51
	37.0	NA	NA	11.59	5.21	14.06	3.90	9.45	5.34

[a] The RSDs for K_a values from the model fitting at 25 and 37 °C for 19 ApoB were 6.8% and 24.7%, respectively, and for 15 ApoE 7.9% and 34.8%, respectively.

heterogeneity around one single type of polar interaction; this polar function was placed in more than one position in the peptide(s). So, the AED-calculations are a good tool for distinguishing between unimodal and multimodal adsorption models. The AED plots here clearly demonstrate that the process is unimodal at both temperatures (see Figure 2C). The main difference is that the monolayer saturation capacity (Δf_{max}, the area of the AED) is much smaller at 37.0 °C than at 25.0 °C. The raw adsorption data fitted to a Langmuir model is presented in Table 1 together with the AED data. As seen, the adsorption isotherm model fitting is in excellent agreement with the AED-calculations; as the temperature was raised it did not affect the energy of interaction (almost unaffected K_a values) but only the monolayer saturation capacity (more than halved Δf_{max}). Thus, the AED-calculations revealed that the energy of interaction was unaffected by the temperature (from 25.0 to 37.0 °C) whereas, interestingly, the access of the 19 amino acid peptide to available adsorption sites was considerably higher at the lower temperature. The acquired adsorption isotherm data for 15 amino acid peptide of ApoE toward C6S is presented in Figure 3A at 25.0 and 37.0 °C. The Scatchard plots (Figure 3B) are nonlinear indicating heterogeneous AED. Models with such Scatchard plots are, e.g., Tóth, bi-Langmuir, etc. To get more detailed information about the adsorption process, the AED was calculated (Figure 3C). The AED was at least bimodal, with an unconverted low energy site and a converted high energy site for both temperatures. Unconverted low energy sites are rather common in adsorption studies,[5,6] because the sample concentration used is too low to sufficiently saturate the low energy adsorption site. Because the AED was bimodal, the Tóth model (unimodal unsymmetrical AED) could not describe the data. The data was therefore instead fitted to the simplest bimodal model (bi-Langmuir), and the AED data and the fitted parameters are presented in Table 1. The low energy adsorption site (site 1) is more or less unaffected by the temperature. The high energy adsorption site (site 2) shows exothermic behavior with decreased adsorption energy with increasing temperature.

It was noticed that 15 amino acid peptide of ApoE with charge of +7 had a stronger interaction toward C6S than 19 amino acid peptide of ApoB with charge of +6 probably due to the stronger electrostatic interactions toward C6S. In addition to electrostatic interactions there are most presumably other minor interactions. It is also possible that the analyte interacts with the surface of the chip. In the experiments a new LNB-carboxyl chip was used, because it can provide less nonspecific binding of the analyte toward the chip surface than normal carboxyl chip. C6S was covalently attached to the chip using amino coupling without losing the negative and reactive groups important in the interactions with peptides.

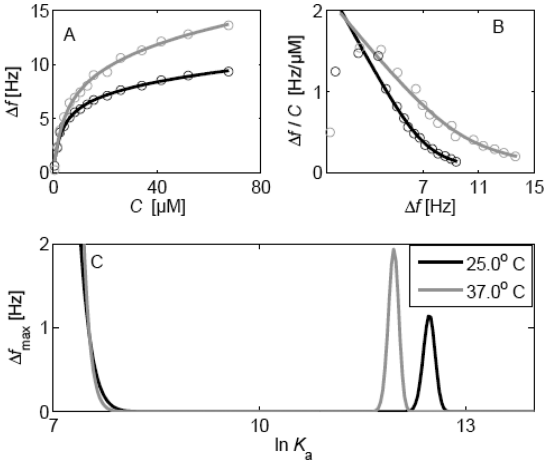

Figure 3. Adsorption isotherm of 15 amino acid peptide of ApoE at 25.0 and 37.0 °C determined (A) using QCM, (B) in corresponding Scatchard plot, and (C) in AED-calculations for this system is presented.

Partial Filling Capillary Electrophoresis. Several capillary electrophoretic methods have been developed for the quantitative assessment of drug−protein interactions. In our recent studies, affinity capillary electrophoresis with partial filling technique applied to the interaction studies between lipoproteins and hydrophobic, neutral steroids under basic conditions proved to be a very promising technique for determination of the affinity of various compounds toward lipoproteins.[15]

In this study the adsorption of positive peptides of apolipoproteins toward the negatives charges of the capillary was minimized by coating the inner capillary wall with acrylamide coating. The coating procedure took only one day, and the coating was stable for a maximum of four days. Electro-osmotic flow mobilities measured by the Williams and Vigh method[28] were in the range 4.5×10^{-6} to 6.1×10^{-6} cm^2/(V s) showing that the minor cationic nature of the capillary resulted in anodic EOF. The repeatability of EOF was used as an indicator for the stability of the coating. RSD% values of run-to-run, day-to-day, and capillary-to-capillary were 2.1%, 3.6%, and 4.7%, respectively.

For the successful interaction study between 19 amino acid peptide of ApoB and 15 amino acid of ApoE with C6S of ECM proteoglycan by affinity capillary electrophoresis with partially filling technique at physiological temperature, the main criteria is that the mobility of partially filled C6S acting as dispersed phase is reverse to those of the peptides. In the slightly cationic copolymer-coated capillary with anodic EOF, the mobility of

dx.doi.org/10.1021/ac201110c |Anal. Chem. 2011, 83, 6040–6046

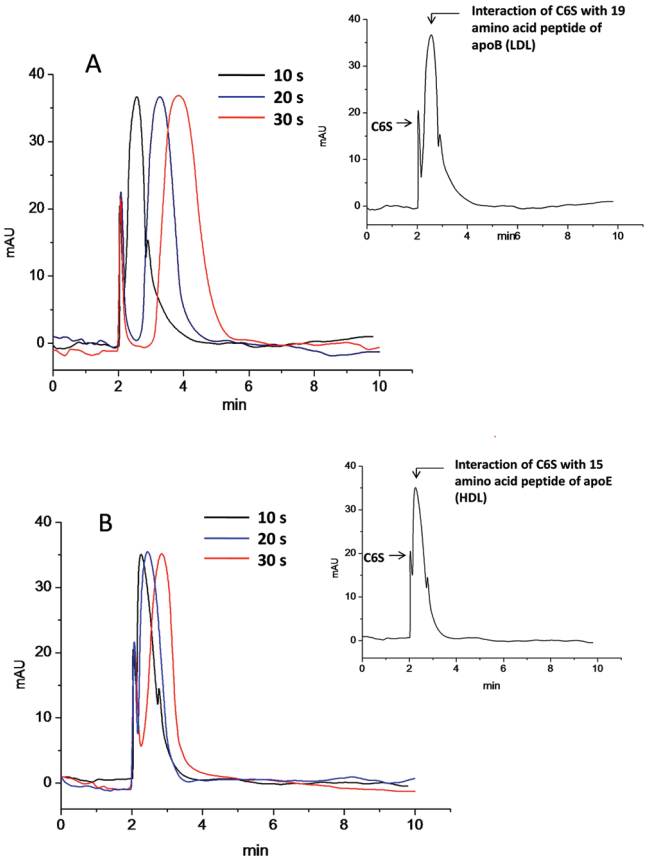

Figure 4. Electropherograms obtained by affinity capillary electrophoresis with partial filled technique are displayed as a function of increased migration time of (A) 19 amino acid peptide of ApoB with increased filling time of C6S (10, 20, and 30 s) and (B) 15 amino acid peptide of ApoE. Running conditions: L_{tot} 38.5 cm, L_{det} 30 cm, internal diameter 50 μm, voltage = −20 kV, capillary temperature 37 °C, detection wavelength 200 nm, peptide solutions (0.01 mg/mL), injection time of peptides 5 s at 50 mbar, C6S solution (1.0 mg/mL), BGE phosphate buffer (I = 20 mM), and pH 7.4.

the positive peptides was lower compared to that in the fused-silica capillary, ensuring that the sample zone of the peptides introduced had sufficient time to pass C6S and interact with them. The effect of C6S filling times from 5 to 40 s and C6S concentrations from 0.001 to 1.0 mg/mL on the interactions in this countercurrent process was studied by affinity capillary electrophoresis. Due to the low sensitivity of the UV detector for sugars, the best results were obtained with the highest concentration 1.0 mg/mL. Moreover, because with a filling time longer than 30 s satisfactory separations were not achieved, filling times of 10, 15, 20, 25, and 30 s were used in all the further studies (Figure 4A,B). The corrected changes of the migration times of the interaction increased linearly with the filling time of the C6S with the correlation coefficients of 0.993 and 0.998 for 15 and 19 amino acids peptides, respectively. The changes in migration times for 19 amino acid peptide were higher than the changes for 15 amino acid peptide. For the quantitative evaluation of the affinity, affinity constants between C6S and the peptides were calculated according to eq 4. On the basis of the affinity constant obtained the interaction between 19 amino acid peptide and C6S was slightly weaker [log K_a 5.02 with RSD of 1.45% (n = 3)] than that between 15 amino acid peptide and C6S [log K_a 5.28 with RSD 1.87% (n = 3)]. Most probably, positive peptides of apolipoproteins were bound to C6S mainly via electrostatic interactions, although some weak site-specific interactions that could not be numerically determined might also play a minor role in interactions.

Molecular Dynamic Simulation Studies. To assess the interaction strength between peptide fragments of ApoB-100 and ApoE and C6S, a free energy calculation was performed through PMF calculation using MD simulations tool. The integrands of the PMF from which K_d were derived are presented for both systems in Figure 5. It is seen that the log K_a value is weakly dependent on the R_c value for r > 0.8 nm for 19 amino acid peptide of ApoB and r > 2.0 nm for 15 amino acid peptide of ApoE. Adequate R_c values were 0.9 and 1.2 nm for 19 amino acid peptide and 1 and 1.7 nm for 15 amino acid peptide (Figure 5). K_d range of 45 nM (log K_a = 7.4) for 19 amino acid peptide and 15−24 μM (log K_a = 4.6) for 15 amino acid peptide proved that both peptides have quite strong interactions toward C6S (Figure 6).

Comparison of Three Approaches. Before results obtained with three approaches are compared, some major differences should be pointed out. With QCM raw adsorption isotherm data is determined, where it is possible to distinguish weak and strong interactions. The affinity coefficient determined PF-ACE is derived assuming a single type of interaction and that the analyte does not affect the free fraction of adsorbent (C6S). This approach will mainly probe the strong adsorption interactions. In MD calculations, short- and long-range interactions can be distinguished because all interactions are taken into account.

The affinity constants obtained with two different experimental techniques, QCM and PF-ACE, agreed quite well, especially when differences between the techniques are kept in mind (Table 2). These affinity constant values are also in very good agreement with the value reported for apoB sequence 3359−3377 linked to lipid vesicles.[6] In the continuous flow QCM with essentially equilibrium processes C6S was covalently immobilized via amino bonding onto the chip surfaces, while in PF-ACE C6S was freely floating in background electrolyte solution leading to slightly lower affinity constant values. In addition, several peptide concentrations were used in QCM for affinity determinations opposite to PF-ACE technique where the peptide concentration was constant while C6S concentrations were enhanced in the experiments. Further, from a time point of view, QCM measurements including optimization procedure took almost three times longer than PF-ACE studies.

Although good agreement was found between three applied methods for 15 amino acid peptide interaction of ApoE toward C6S as seen from Table 2, molecular dynamic simulation studies provided slightly higher affinity constant value for 19 amino acid peptide of ApoB.

In the molecular dynamics simulation the molecules are able to relax freely with no time constraints other than the extendable simulation time, and one possible explanation for higher interaction strength compared to experimental results is the relaxation time. This is assuming 19 amino acid peptide of ApoB needs more time to fully interact with C6S than the smaller peptide fragment of ApoE. However, longer interaction time was not realized, nor physiological salt concentration of 200 mM in the QCM and PF-ACE studies. In addition, we should keep in mind that helical secondary structures were assumed for both peptides, although helical structure appears not to be a prerequisite for the optimum interaction between ApoE and C6S (Figure 6), opposite to the interaction between ApoB and C6S as demonstrated in our most recent study.[18] Moreover, steric effects that might be present in the experiments due to concentration effect of analyte

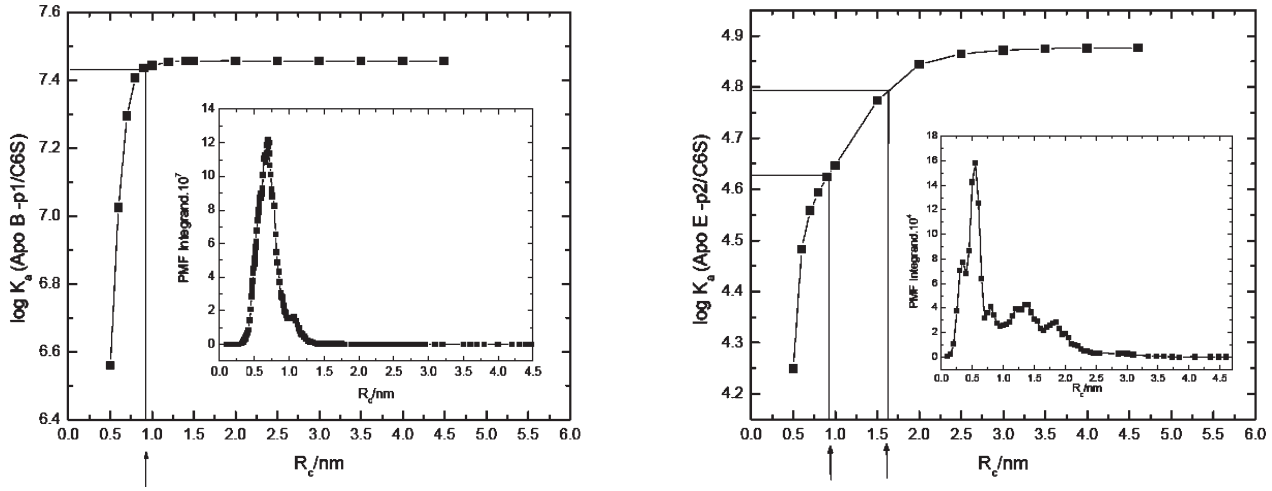

Figure 5. Logarithm of the association constant K_a as function of R_c[24] (limit for association). The integrand of the potential of mean force (PMF) is included as inset in the plot.

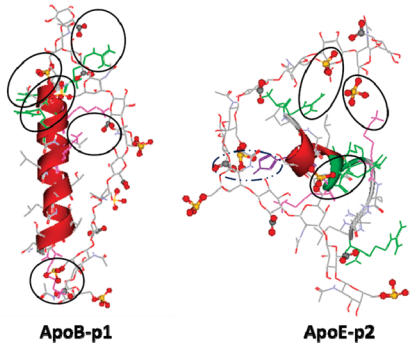

Figure 6. Snapshots of 19 amino acid peptide of ApoB/C6S and 15 amino acid peptide ApoE/C6S at the peak of the PMF integrand. Color code: arginine in green, lysine in pink, and histidine in purple. Representations: C6S in line from which carboxylate and sulfate groups are in ball stick representation. Solid ribbons are for the peptides. Salt bridges are indicated by black circles.

Table 2. Log K_a Values Obtained for 19 Amino Acid Peptide of ApoB and 15 Amino Acid Peptide of ApoE with Quartz Crystal Microbalance, Affinity Capillary Electrophoresis with Partial Filling Technique (PF-ACE) and Molecular Dynamic Simulations (MDS) (For comparison some log K_a values found in literature are given.[6])[a]

peptide	T [°C]	log K_a QCM	log K_a PF-ACE	log K_a MDS	log K_a (ref)
19 aa of ApoB	25.0	4.65[1] (4.62**)			
19 aa of ApoB	37.0	4.66[1] (4.64**)	5.02	7.39	4.7[b] (ref 6)
					5.4[c] (ref 6)
15 aa of ApoE	25.0	5.51[2] (5.42**)			
15 aa of ApoE	37.0	5.34[2] (5.21**)	5.28	4.60	

[a] 1 indicates Langmuir; 2 indicates bi-Langmuir r, **AED = adsorption energy distribution. [b] Value for ApoB (3359−3367)/C6S interaction. [c] Value for ApoB(3359−3367) associated with lipid vesicles/C6S interaction.

may also affect the secondary/tertiary structure of the 19 amino acid peptide and influence its interaction.

CONCLUSIONS

Two different experimental techniques, namely continuous flow QCM and partially filling affinity capillary electrophoresis, were applied to the determination of the affinity between LDL and HDL and C6S of proteoglycan. Because the association of ApoB of LDL and ApoE of HDL with the arterial PG is mediated by specific highly positive peptide fragments of apolipoprotein, 19 amino acid peptide and 15 amino acid peptide with arginine and lysine amino acid rich components were selected for interaction studies. In the third approach molecular dynamics simulation calculations were used to complete the studies.

For a more detailed understanding of the adsorption processes the adsorption isotherms were determined over a wide concentration range to be able to probe weak as well as strong interactions. The slopes of the Scatchard plot were nearly identical for 19 amino acid peptide of ApoB toward C6S indicating that the adsorption energies at both temperatures were similar. The AED-calculations that aimed at detailing the adsorption processes demonstrated the binding process to be unimodal at both temperatures 25.0 and 37.0 °C, and confirmed that the adsorption energies were similar at both temperatures. Further, the AED-calculations revealed that the monolayer saturation capacity was much smaller at 37.0 °C than at 25.0 °C. Thus, the AED-calculations proved that the energy of interaction is unaffected by the temperature whereas the access of the 19 amino acid peptide to available adsorption sites was considerably higher at the lower temperature.

For 15 amino acid peptide of ApoE toward C6S the AED-calculations showed that the interactions can be lumped to a bimodal distribution comprising two different adsorption sites. The data fitted very well to the simplest bimodal model (bi-Langmuir), and the AED data and the fitted parameters agreed excellently. The low energy adsorption site was more or less unaffected by the temperature while the high energy adsorption site showed exothermic behavior. The developed technique has a great potential for the determination of the affinity of various compounds toward lipoproteins.

In electrophoresis the coated capillaries were partially filled with C6S, which acted as dispersed phase. The filling time and C6S concentration were optimized to get reliable affinity constants that agreed very well with the strong association equilibrium

dx.doi.org/10.1021/ac201110c |Anal. Chem. 2011, 83, 6040–6046

constants determined by QCM. PF-ACE was a much faster method than QCM, but it enables only the determination of strong interactions. Because the determination of adsorption isotherms by QCM does not assume any model, both weak and strong adsorption interactions could be determined. Even complicated nonideal adsorption processes such as adsorbate–adsorbate interactions and multilayer adsorption could be determined. The limiting factor in QCM is the quality of the determined adsorption data.

Our earlier designed and validated force field for a C6S dodecasaccharide chain was successfully used to unravel the interactions between peptide residues of ApoB and ApoE and C6S. Molecular dynamic simulation studies acted as an excellent computational tool in the affinity studies supporting the results achieved with the experimental techniques.

■ ASSOCIATED CONTENT

Supporting Information. Additional information as noted in text. This material is available free of charge via the Internet at http://pubs.acs.org.

■ AUTHOR INFORMATION

Corresponding Author

*E-mail: Marja-Liisa.Riekkola@helsinki.fi.

■ ACKNOWLEDGMENT

Professor Petri T. Kovanen and Dr. Katariina Öörni from the Wihuri Research Institute, Helsinki, Finland, are thanked for valuable discussions. Financial support was provided by the Research Council for Natural Sciences and Engineering of the Academy of Finland under Grants 116288 and 1133184 (K.L., G.C., P.W.S., and M.-L.R.), and by the National Scientific and Technical Research Council (CONICET), Argentina (P.W.S.). The CSC-IT center for Science is thanked for allocating CPU time and supercomputer resources. Particular acknowledgment is given to Dr. Atte Sillanpää for his valuable help for the pull code calculations. The authors (T.F. and J.S.) also acknowledge a grant from the Swedish Research Council (VR): "Fundamental Studies on Molecular Interactions Aimed at Preparative Separations and Biospecific Measurements".

■ REFERENCES

(1) Camejo, G. *Adv. Lipid Res.* **1982**, *19*, 1–53.
(2) Williams, K. J.; Tabas, I. *Arterioscler., Thromb., Vasc. Biol.* **1995**, *15*, 551–561.
(3) Radhakrishnamurthy, B.; Srinavasan, P.; Vijayagopal, P.; Berenson, G. S. *Eur. Heart J.* **1990**, *11*, 148–157.
(4) Camejo, G.; Olofsson, S.-O.; Lopez, F.; Carlsson, P.; Bondjers, G. *Arteriosclerosis* **1988**, *8*, 368–377.
(5) Camejo, G.; Rosengren, B.; Olson, U.; Lopez, F.; Olofson, S. O.; Westerlund, C.; Bondjers, G. *Eur. Heart J.* **1990**, *11*, 164–173.
(6) Olsson, U.; Camejo, G.; Bondjers, G. *Biochemistry* **1993**, *32*, 1858–1865.
(7) Alavl, M. Z.; Moore, S. *Atherosclerosis* **1987**, *63*, 65–74.
(8) Srinivasan, S. R.; Vijayagopal, P.; Dalferes, E. R.; Abatte, B.; Radhakrishnamurthy, B.; Berenson, G. S. *Atherosclerosis* **1986**, *62*, 201–208.
(9) D'Ulivo, L.; Saint-Guirons, J.; Ingemarsson, B.; Riekkola, M.-L. *Anal. Bioanal. Chem.* **2010**, *396*, 1373–1380.
(10) Vainikka, K.; Reijmar, K.; Yohannes, G.; Samuelsson, J.; Edwards, K.; Riekkola, M.-L. *Anal. Biochem.* **2011**, *414*, 117–124.
(11) Stanley, B. J.; Guiochon, G. *J. Phys. Chem.* **1993**, *97*, 8098–8104.
(12) Samuelson, J.; Franz, A.; Stanley, B. J.; Fornstedt, T. *J. Chromatogr., A* **2007**, *1163*, 177–189.
(13) Gritti, F.; Guiochon, G. *J. Chromatogr., A* **2005**, *1099*, 1–42.
(14) Sandblad, P.; Arnell, R.; Samuelsson, J.; Fornstedt, T. *Anal. Chem.* **2009**, *81*, 3551–3559.
(15) Wang, A.-J.; Vainikka, K.; Witos, J.; D'Ulivo, L.; Cilpa, G.; Öörni, K.; Kovanen, P. T.; Jauhiainen, M.; Riekkola, M.-L. *Anal. Biochem.* **2010**, *399*, 93–101.
(16) Cifuentes, A.; Díez-Masa, J. C.; Fritz, J.; Anselmetti, D.; Bruno, A. E. *Anal. Chem.* **1998**, *70*, 3458–3462.
(17) Cilpa, G.; Koivuniemi, A.; Hyvönen, M. T.; Riekkola, M.-L. *J. Phys. Chem. B* **2011**, *115*, 4818–4825.
(18) *Accelrys Discovery Studio 2.1*; Accelrys: San Diego, CA; http://www.accelrys.com.
(19) Hess, B.; Kutzner, C.; Van der Spoel, D.; Lindahl, E. *J. Chem. Theory Comput.* **2008**, *4*, 435–447.
(20) Cilpa, G.; Hyvönen, M. T.; Koivuniemi, A.; Riekkola, M.-L. *J. Comput. Chem.* **2010**, *31*, 1670–1680.
(21) Bussi, G.; Donadio, D.; Parrinello, M. *J. Chem. Phys.* **2007**, *126*, 014101.
(22) Bussi, G.; Zykova-Timan, T.; Parrinello, M. *J. Chem. Phys.* **2009**, *130*, 074101.
(23) Berendsen, H. J. C.; Postma, J. P. M.; van Gunsteren, W. M.; DiNola, A.; Haak, J. R. *J. Chem. Phys.* **1984**, *81*, 3684–3690.
(24) Justice, M.-C.; Justice, J.-C. *J. Solution Chem.* **1976**, *5*, 543–547.
(25) Zhang, Y.; McCammon, J. A. *J. Chem. Phys.* **2003**, *118*, 1821–1827.
(26) Pei, Y.; Yu, H.; Pei, Z.; Theurer, M.; Ammer, C.; Andr, S.; Gabius, H.-J.; Yan, M.; Ramström, O. *Anal. Chem.* **2007**, *79*, 6897–6902.
(27) Zhang, X.; Samuelsson, J.; Janson, J.-C.; Wang, C.; Su, Z.; Gu, M.; Fornstedt, T. *J. Chromatogr., A* **2010**, *1217*, 1916–1925.
(28) Williams, B. A.; Vigh., G. *Anal. Chem.* **1996**, *68*, 1174–1180.

■ NOTE ADDED AFTER ASAP PUBLICATION

This paper was published on the Web on June 24, 2011, with an error in the Abstract and a change in the presentation of Table 2 footnotes. The corrected version was reposted on June 29, 2011.